

Hyperspectral Change Detection using Multi-temporal Hyperspectral images and Sparse Unmixing algorithm

¹Nareshkumar Patel ²Himanshukumar Soni

¹Department of Electronics and Communication Engineering,
Sarvajani College of Engineering and Technology, Surat-395001, Gujarat, India.

²Department of Electronics and Communication Engineering
G. H. Patel College of Engineering and Technology, V. V. Nagar, Anand-388120, Gujarat, India.

¹Orcid id: 0000-0001-7806-0087

Abstract

Hyperspectral Change Detection (HCD) is the process of obtaining information about the changes in the abundance map of materials present in scene using multi-temporal Hyperspectral Images of Instantaneous Field Of View (IFOV) under observation. Multi-temporal Images are taken by a Hyperspectral Camera (HSC) at different time and may be at different environmental conditions. The information regarding changes in their IFOV can be useful for variety of applications like environmental monitoring, city planning, military surveillance and disaster management and etc. HSC measures the Electro-Magnetic (EM) radiation at more than 200 narrow and contiguous bands in their IFOV. Three dimensional image captured by HSC has two spatial and one spectral dimension. Spectral dimension covers the visible, near-infrared, and shortwave infrared spectral bands (0.3-2.5 μm) of electromagnetic spectrum with very high spectral resolution of 10nm. Linear Spectral Unmixing (LSU) is widely used technique in the field of Remote Sensing (RS) for the estimation of number of materials, known as endmembers, their fractional proportion, known as abundance maps and their spectral signatures. The Sparse Regression (SR) based approach, the best solution for LSU in semi-supervised manner, assumes the availability of some standard publically available spectral libraries, which contains spectral signatures of many materials measured on the earth surface using advance spectro-radiometer. In SR based approach the problem of LSU is simplified to finding the optimal subset of spectral signatures from the spectral library known in advance. High spectral resolution of HSI and advent of Sparse Unmixing (HU) algorithms are capable of finding small variations in Hyperspectral images. In this paper, Sparse Unmixing using variable Splitting and Augmented Lagrangian (SUnSAL) is used for change detection for multi-temporal Hyperspectral images. Simulation results conducted with the help of synthetically generated data cubes, using HYDRA tool, validates the performance of SUnSAL for change detection application.

Keywords: Hyperspectral Unmixing, Linear Mixing Model, Linear Spectral Unmixing, Sparse Unmixing, Sparse Regression, SUnSAL, Change Detection

1. INTRODUCTION

The process of detecting sub pixel level variations from the scene under observation using multi-temporal hyperspectral images is known as Hyperspectral Change Detection in the field of Remote Sensing (RS). The changes in scene may be due to seasonal variation, natural disaster or as time. HCD enables variety of application like natural disasters monitoring on earth surface, military target movement detection, crop assessment, disaster management, urban planning [1][2]. Reflection, emitting and absorption characteristics of all substances are a function of wavelength of Electromagnetic (EM) spectrum. The reflection vs. wavelength plot is known as spectral signature of substance and it is used to identify the materials. [2]. In HSI, the number of substances present is known as endmembers. The fractional proportion of endmembers in image is known as abundance map. The process of estimating number of endmembers, their spectral signatures and their abundance map is challenging task. Various algorithms have been proposed till date to manage the problem of Linear Spectral Unmixing (LSU)[4][5]. Geometrical and Statistical approach based algorithms assumes that only hyperspectral data cube is available for LSU[5]. In Sparse Regression (SR) approach based algorithm assumes that observed spectral signature of pixel may be represented as linear mixing of few spectral signatures from Spectral Library [6].

Several traditional methods like Chronochrome (CC), Covariance Equalization (CE) were founds in literature do not provide intra pixel information [1][3]. In Hyperspectral images changes occur within pixel due to very poor spatial resolution so the traditional methods do not provide accurate results for change detection. LSU is emerged as powerful technique in the field of RS to get information up to sub pixel level. Recently several researchers have proposed different techniques for change detection or anomaly detection from Hyperspectral images using various spectral unmixing algorithms. Recently the techniques for anomaly detection using Vertex Component Algorithm (VCA) for multi-temporal hyperspectral images have been proposed [2]. Various sparse unmixing based algorithms have been proposed in last few years [9] [10]. In this paper for change detection, sparse unmixing is performed by SUnSAL [11] on horizontally concatenated hyperspectral images. The performance of verified with the help of synthetically

generated multi temporal hyperspectral image using HYDRA tool. LSU is more robust and gives accurate results when there are changes within pixels[12].

2. HYPERSPECTRAL IMAGE FORMATION MODEL

For each single pixel of three dimensional hyperspectral data cube the LMM can be written as

$$y_i = \sum_{j=1}^q m_{ij}x_j + n_i \quad (1)$$

Where the subscript i represents the spectral band number and subscript j represents the endmember number from endmember matrix M . The length of observed vector y is L , i.e. $i=1, 2 \dots L$. and number of endmembers in endmember matrix are q , i.e. $j=1, 2 \dots q$. For j th endmember of endmember matrix M , the reflectance at band i is represented as m_{ij} and the fractional proportion in a pixel is given by x_j . In general, mathematically LMM can be written for one pixel in compact form as

$$y = Mx + n \quad (2)$$

Where $y \in R^L$ is an observed spectral vector, $M \in R^{L \times q}$ is endmember matrix and $x \in R^q$ is fractional abundances map of the endmembers for a given pixel, and $n \in R^L$ is the error term.

The value of fractional abundance is always nonnegative, lie in the range of 0 to 1 and sum of its values for single pixel is always one. The constraints are represented in compact form as $x_j \geq 0$ and $\sum_{j=1}^q x_j = 1$.

3. CHANGE DETECTION USING SUnSAL

In Sparse Unmixing (SU) endmembers are not extracted from hyperspectral data cube to solve LSU problem but endmembers are selected from spectral library. Spectral library contains thousands of spectral signatures recorded in advance on the earth surface using spectro radiometer [6]. For sparse unmixing searching operation must be conducted in a standard library, $A \in R^{L \times m}$, where L is the number of bands and m is the number of endmembers in the library. Usually, the number of spectral signatures are much larger than spectral bands in standard library, i.e., $L \ll m$. Let vector, $x \in R^m$, denotes the fraction abundance map for given pixel related to the library A . Let us assume that out m materials available in A , less than k materials are present in the scene, where $k \ll m$. So we can say that x is k -sparse vector because most of component of vector are zero. Figure 3 shows the sparse regression based approach for Hyperspectral unmixing [6].

Two standard spectral libraries are available online for research work, USGS and ASTER [6][13].

The LSU problem as per sparse regression approach can be written as

$$\min_X \|AX - Y\|_F^2 + \lambda \|X\|_{1,1} + l_{R+}(X) \quad (3)$$

Where $l_{R+}(X) = \sum_{i=1}^n l_{R+}(x_i)$ is the indicator function (x_i represents the i th column of X and $l_{R+}(x_i)$ is zero if x_i belongs to the nonnegative orthant and $+\infty$ otherwise).

With the use of variable splitting concept the function written in eq (3) can be given as

$$\min_{U, V_1, V_2, V_3} \frac{1}{2} \|V_1 - Y\|_F^2 + \lambda \|V_2\|_{1,1} + l_{R+}(V_3) \quad (4)$$

Subject to $V_1 = AU, V_2 = U, V_3 = U$

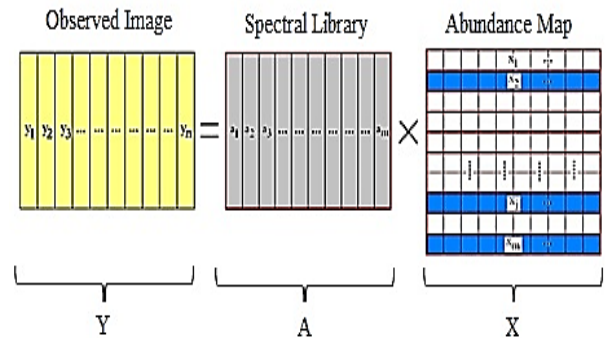


Figure 1. Sparse Regression based approach for Linear Spectral Unmixing [9]

In compact form

$$\min_{U, V} g(V) \quad (5)$$

Subject to $GU + BV = 0$

Where $g(V) = \frac{1}{2} \|V_1 - Y\|_2^2 + \lambda \|V_2\|_1 + l_{R+}(V_3)$ (6)

In which $V = (V_1, V_2, V_3)$

Let,

$$\begin{aligned} V_1 = AU &\Rightarrow AU - V_1 = 0 \\ V_2 = U &\Rightarrow U - V_2 = 0 \\ V_3 = U &\Rightarrow U - V_3 = 0 \end{aligned} \quad (7)$$

Eq (7) in matrix form,

$$G = \begin{bmatrix} A \\ I \\ I \end{bmatrix} \quad B = \begin{bmatrix} -I & 0 & 0 \\ 0 & -I & 0 \\ 0 & 0 & -I \end{bmatrix}$$

The Augmented Lagrangian for eq. (5) is written as

$$\mathcal{L}(U, V, D) = g(U, V) + \frac{\mu}{2} \|GU + BV - D\|_2^2 \quad (8)$$

subject to $GU + BV = 0$

Expansion of eq. (8) can be rewritten as eq. (9)

$$\mathcal{L}(U, V_1, V_2, V_3, D_1, D_2, D_3) = \frac{1}{2} \|V_1 - Y\|_2^2 + \lambda \|V_2\|_{1+\text{R}^+}(V_3) + \frac{\mu}{2} \|AU - V_1 - D_1\|_2^2 + \mu \|U - V_2 - D_2\|_2^2 + \frac{\mu}{2} \|U - V_3 - D_3\|_2^2 \quad (9)$$

The ADMM is applied to eq. (9) to solve the optimization. The detailed description of SUnSAL is discussed in [6], [10]. The pseudo code for SUnSAL is given as below.

Algorithm: ADMM pseudo code for solving SUnSAL problem [6]

Initialization: set $k = 0$, choose $\mu > 0, U^{(0)}, V^{(0)}, D^{(0)}$,

Repeat:

$$U^{(k+1)} \leftarrow (A^T A + 2I)^{-1} (A^T (V_1^{(k)} + D_1^{(k)}) + (V_2^{(k)} + D_2^{(k)}) + (V_3^{(k)} + D_3^{(k)}))$$

$$V_1^{(k+1)} \leftarrow \frac{1}{1+\mu} [Y + \mu (AU^{(k)} - D_1^{(k)})]$$

$$V_2^{(k+1)} \leftarrow \text{soft}((U^{(k+1)} + D_2^{(k)}), \frac{\lambda}{\mu})$$

$$V_3^{(k+1)} \leftarrow \max(U^{(k)} - D_3^{(k)}, 0)$$

$$D_1^{(k+1)} \leftarrow D_1^{(k)} - AU^{(k+1)} + V_1^{(k+1)}$$

$$D_2^{(k+1)} \leftarrow D_2^{(k)} - U^{(k+1)} + V_2^{(k+1)}$$

$$D_3^{(k+1)} \leftarrow D_3^{(k)} - U^{(k+1)} + V_3^{(k+1)}$$

until some stopping criteria is satisfied

In this work, we assume that both images are atmospherically corrected and captured under the same circumstances. Two images, taken by single camera but at different time, are horizontally concatenated to form as single image with doubled pixels. Now the sparse unmixing is performed on a single image to estimate the fractional abundance map as described in pseudo code. Then estimated fraction abundance map is separated into fractional abundance maps for original image and changed image as shown in fig (2).

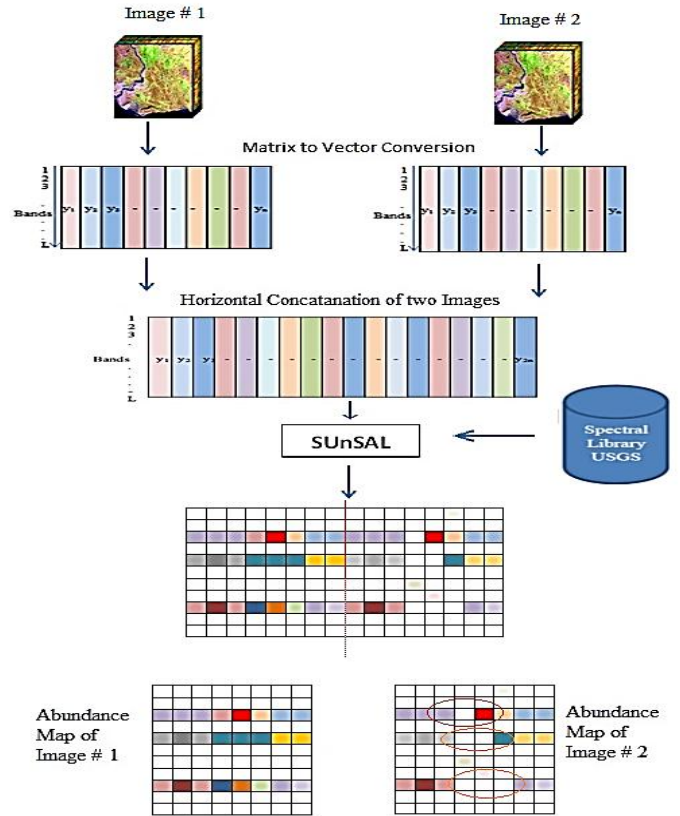
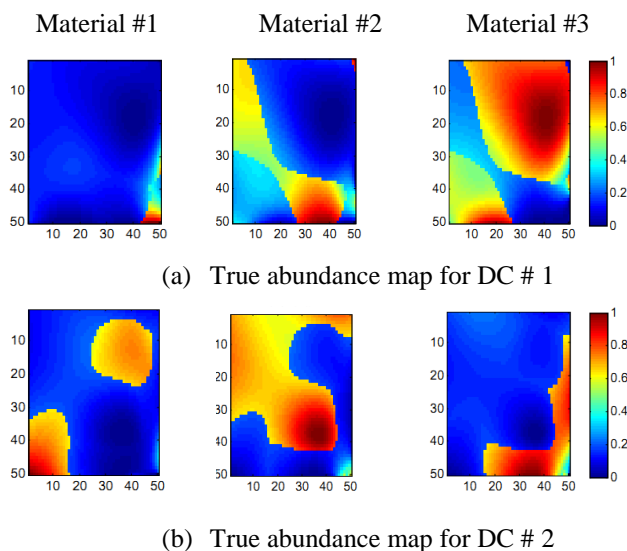
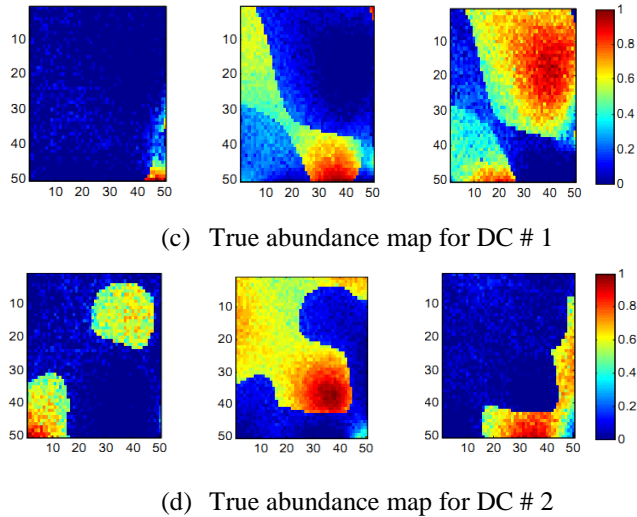


Figure 2. Change Detection Mechanism using SUnSAL

4. SIMULATION RESULTS AND DISCUSSION

In this section, to demonstrate the application of change detection using multi-temporal hyperspectral data we have used synthetically generated Hyperspectral images taken at different time due to non-availability of real data set of multi temporal Hyperspectral images. The resultant data cubes are then corrupted with Gaussian Noise with different values of SNR. Three spectral signatures, namely Alunite GDS84





number of pixels will be doubled, $2N$, in input image for sparse unmixing process. Now the size of fractional abundance map X used for sparse unmixing will be $P \times 2N$. Fig 3 (c) and (d) shows the estimated fractional abundance for $DC \#1$ and $DC \#2$. After comparison of estimated abundance map for both DCs user can know about the changes occur in fractional proportion of material in the scene.

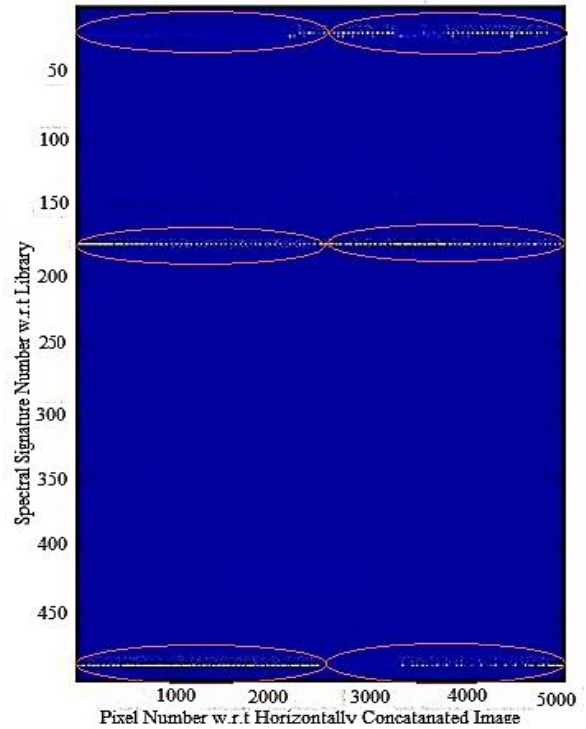


Figure 3.(a)&(b) True Abundance map for Data cube # 1 and 2. (c) & (d) Estimated Abundance map for Data Cube # 1 and 2. True and Estimated Fractional Abundance map

Figure 4. Estimated Fractional abundance map for Concatenated Data cubes

NaO3, Diaspore HS416.3B and Dry long grass AV87-2, are selected from library database to create hyperspectral data cube. The subset of the USGS spectral library contains 498 spectral signatures and denoted by A . Selected Spectral signatures are stored in measurement matrix M . The size of data cube is kept 50×50 and we have assumed that only three materials from the measurement matrix are present in data cube. To show the variation in scene two sets of abundance map are generated. Fig 3(a) and (b) shows the fractional abundance map for $DC \#1$ and $DC \#2$ respectively. Fractional abundance maps are generated using the spherical Gaussian field as available in the HYDRA package [14]. As per Linear Mixing Model (LMM) for hyperspectral image formation, as discussed in section 2, $DC \#1$ of size $50 \times 50 \times 224$ is generated using measurement matrix M and fractional abundance maps as shown in fig 3(a). In order to generate the data corresponding to different time instant, we use the same set of endmembers but with different abundances as shown in fig3(b). Similarly another data cube of same size, denoted as $DC \#2$, is generated. $DC \#1$ and $DC \#2$ show the possible temporal variation in its IFOV of HSC over a given period of time.

Fractional abundance map for horizontally concatenated DCs are shown in Fig (4). The vertical axis indicates the spectral signature number with respect to spectra library and horizontal axis indicates the pixel number of horizontally concatenated data cubes. In this simulation we have taken two data cube of size 50×50 . So, total number of pixels in horizontally concatenated data cubes will be 5000. First 2500 pixels are corresponds to first data cubes and remaining 2500 pixels corresponds to second data cube. From the fig (4), it is seen that only three materials are present in both DCs. It is also seen that the fractional abundance maps are not same for these three materials in two data cubes. Difference in fractional abundance map of material is considered as change in hyperspectral data cube and it is highlighted with red colour circles.

In sparse unmixing of hyperspectral data first fractional abundance map of materials are estimated and then spectral signatures are selected from the spectral library. As shown in fig. (2), each DC is converted into $L \times N$ Matrix, where N is the number of pixels in DC and each column of matrix represents the spectral signature of corresponding pixel. According to the size of DC, we assume the size of the abundance map as $P \times N$ matrix. The j th row of abundance map matrix indicates the proportion of j th material from spectral library in all pixels of scene. Change detection is performed using synthetic data cubes ($DC \#1$ and $DC \#2$) and spectral A , as per methodology discussed in section 3. For change detection using sparse unmixing, two images are horizontally concatenated as shown in fig. 2. Now the

Different sets of data cube are generated using HYDRA tool to validate the performance of SUNSAL algorithm for change detection application. Other sets of data cubes are generated with same size but endmembers are taken as 5 and 9.

5. CONCLUSION

Due to very poor spatial resolution of hyperspectral image the change in material fractional proportion will occur at sub pixel level. So change detection algorithms used for normal images cannot be used to detect change from multi-temporal hyperspectral images. LSU is the most efficiently performed in sparse regression based technique to get information up to sub pixel level. In SU of Hyperspectral data approach unmixing is simplified to finding the optimal subset of endmember signature from the library. Complexity of Sparse Unmixing via variable splitting and augmented lagrangian (SUnSAL) is reduced with help of ADMM and Augmented Lagrangian. SUnSAL gives more accurate results due to the availability of spectral libraries. Direct comparison of algorithm from SR based approaches is not possible with other algorithm. Simulation results show that SUnSAL can be used for Change detection and it enables variety of application.

REFERENCES

- [1] Ertürk, A., et al., "Hyperspectral change detection by sparse unmixing with dictionary pruning." In IEEE 7th Workshop on Hyperspectral Image and Signal Processing: Evolution in Remote Sensing (WHISPERS), pp. 1-4, June 2016.
- [2] N. Patel and H. Soni, "Anomaly detection using VCA algorithm for multi-temporal hyperspectral images," IEEE International Conference on Wireless Communications, Signal Processing and Networking (WiSPNET), Chennai, 2017, pp. 2248-2252.
- [3] A. Ertürk and A. Plaza, "Informative change detection by unmixing for hyperspectral images", IEEE Geoscience and Remote Sensing Letters, vol. 12, no. 6, pp. 1252-1256, June 2015.
- [4] Keshava, N. and Mustard, J.F., "Spectral unmixing," IEEE Signal Processing Magazine, vol.19, no.1, pp.44,57, Jan 2002.
- [5] Bioucas-Dias, J.M., et al., "Hyperspectral Unmixing Overview: Geometrical, Statistical, and Sparse Regression-Based Approaches," IEEE Journal of Selected Topics in Applied Earth Observations and Remote Sensing, vol.5, no.2, pp.354,379, April 2012.
- [6] M. D. Iordache, et al., "Sparse Unmixing of Hyperspectral Data," IEEE Transactions on Geoscience and Remote Sensing, vol. 49, no. 6, pp. 2014-2039, June 2011
- [7] Y. Elhadad, S. R. Rotman and D. Blumberg, "Analysis of hyperspectral anomaly change detection algorithms," 2016 8th Workshop on Hyperspectral Image and Signal Processing: Evolution in Remote Sensing (WHISPERS), Los Angeles, CA, 2016, pp. 1-5.
- [8] Nascimento, J.M.P. and Bioucas Dias, J.M., "Vertex component analysis: a fast algorithm to unmix hyperspectral data," IEEE Transactions on Geoscience and Remote Sensing, vol.43, no.4, pp.898,910, April 2005
- [9] M. D. Iordache, et al., "Collaborative Sparse Regression for Hyperspectral Unmixing," IEEE Transactions on Geoscience and Remote Sensing, vol. 52, no. 1, pp. 341-354, Jan. 2014.
- [10] M.-D. Iordache, J. M. Bioucas-Dias, A. Plaza, "Total variation spatial regularization for sparse hyperspectral unmixing", IEEE Transactions on Geoscience and Remote Sensing, vol. 50, no. 11, pp. 4484-4502, Nov. 2012
- [11] J. M. Bioucas-Dias and M. A. T. Figueiredo, "Alternating direction algorithms for constrained sparse regression: Application to hyperspectral unmixing," 2nd Workshop on Hyperspectral Image and Signal Processing: Evolution in Remote Sensing, Reykjavik, 2010, pp. 1-4.
- [12] Ertürk, A., et al., "Sparse unmixing-based change detection for multitemporal hyperspectral images", IEEE Journal of Selected Topics in Applied Earth Observations and Remote Sensing, vol. 9, no. 2, pp. 708—719, 2016.
- [13] [online] Available: <http://speclab.cr.usgs.gov/spectral-lib.html>.
- [14] Hyperspectral Imagery Synthesis (EIAs) toolbox. Grupo de Inteligencia Computacional, Universidad del País Vasco/Euskal Herriko Unibertsitatea (UPV/EHU), Spain.
[online] Available: http://www.ehu.es/ccwintco/index.php/Hyperspectral_Imagery_Synthesis_tools_for_MATLAB.